

Chapter 9

Chemical Vapor Deposition of Ca–P–O Film Coating

Takashi Goto and Hirokazu Katsui

Abstract Ca–P–O system bio-ceramic films were coated by chemical vapor deposition (CVD). CVD is a versatile technique for controlling crystal phase and microstructure, which significantly affect bio-compatibility. By introducing auxiliary energy, laser and plasma, in CVD, much wider range of Ca–P–O coatings can be synthesized. Hydroxyapatite regeneration of the Ca–P–O coatings prepared by CVD techniques were evaluated in a simulated body fluid (SBF).

Keywords Apatite regeneration • Calcium phosphate • Crystal structure • Laser and plasma CVD

9.1 Introduction

Metallic bio-materials, typically Ti and Ti alloys, can be used as artificial bones or dental implants because they are non-allergenic, have good corrosion resistance in the human body and possess comparable mechanical properties with bone. However, these metallic bio-materials do not have sufficient tissue compatibility; therefore, they require a few months for bone-regeneration. Since human bone is similar in makeup calcium hydroxyapatite ($\text{Ca}_{10}(\text{PO}_4)_6(\text{OH})_2$) ceramics, materials of the Ca–P–O system are commonly used as bio-ceramic coatings on metallic bio-materials to accelerate the bone regeneration. Several coating techniques, such as plasma spray, sol–gel, alkaline treatment and magnetron sputtering, have been proposed [1]. Although chemical vapor deposition (CVD) has been widely used to prepare various forms of materials, i.e., films, powders and bulks as electric devices and anti-abrasive coatings [2], CVD has rarely been used to synthesize bio-ceramic coatings. However, CVD has advantages in controlling crystal phase and microstructure, providing well-adhered coatings even on complex-shaped metal substrates. CVD is a promising technique for the preparation of bio-ceramic coatings because it can optimize their microstructure to enhance bio-compatibility. The authors of this review have prepared Ca–Ti–O [3], Ca–Si–O [4] and Ca–P–O

T. Goto (✉) • H. Katsui

Institute for Materials Research, Tohoku University, 2-1-1, Katahira, Aoba-ku,
Sendai 980-8579, Japan

e-mail: goto@imr.tohoku.ac.jp

bio-ceramic coatings [5] by CVD. This review briefly describes the CVD preparation of Ca–P–O bio-ceramic coatings and their bone (hydroxyapatite) regeneration behavior in a simulated body fluid (SBF).

9.2 Chemical Vapor Deposition (CVD)

In CVD, various forms of materials (powder, amorphous, poly-crystalline, single-crystal, film and bulk) are prepared through chemical reactions, such as thermal decomposition, hydrolysis and hydrogen reduction. By controlling deposition parameters, i.e., source gases, deposition temperature, gas pressure, geometry of the CVD reaction chamber etc., wide-ranging oxide, nitride, carbide and boride materials with different microstructures (fine grains, cauliflower grains and columnar grains) can be prepared. Since source gases can be easily purified, deposited materials can also be highly pure and dense or intentionally porous. Chemical reactions in CVD take place usually by thermal energy. Therefore, conventional CVD is called thermal CVD. Substrate materials may be degraded and corroded by the high temperature of thermal CVD; auxiliary energy sources such as plasma and laser can be introduced to enhance the chemical reactions and lower the deposition temperature. These CVDs are called laser CVD (LCVD) [6] and plasma-enhanced CVD (PECVD) [7]. Figure 9.1a–c schematically depict thermal CVD, PECVD and LCVD, respectively. In thermal CVD, chemical reactions proceed on a substrate surface, forming films via nucleation and grain growth on the atomic/molecular level. The resulting films are generally well-adhered to the substrate with good step coverage. By optimizing deposition parameters, high deposition rates of 1–2 mm/h can be achieved, forming thick film or bulky materials [8]. Bio-ceramic oxide films are not usually deposited at high deposition rate because precursor vapors and oxygen gas are easily reacted in the gas phase to form powders and premature reactions take place on CVD chamber walls. The deposition rates of oxide films by thermal CVD are commonly around a few $\mu\text{m/h}$ [9]. Thermal CVD can be performed close to thermal equilibrium. The films can be synthesized according to a phase diagram, producing thermally stable products.

PECVD (Fig. 9.1a) uses plasma as an auxiliary energy source. An electromagnetic field with radio frequency (RF: 13.5 MHz) or micro-wave (2.45 GHz) can be applied to a deposition zone to form the plasma. The gas can be discharged and dissociated to activate ions, radicals and electrons. These activated species are significantly reactive, even at low temperatures, forming non-equilibrium or quasi-equilibrium films [10]. The authors first utilized PECVD for preparing bio-ceramic coatings as shown later.

Lasers can be an auxiliary energy source of light and heat in CVD, and thus LCVD (Fig. 9.1c) can be categorized into two types: photolytic LCVD and pyrolytic LCVD [6]. Since a source gas may absorb a specific laser wavelength, photolytic LCVD can prepare films without substrate heating. The laser passes through a gas phase, directly decomposing source gases. Photolytic LCVD using a

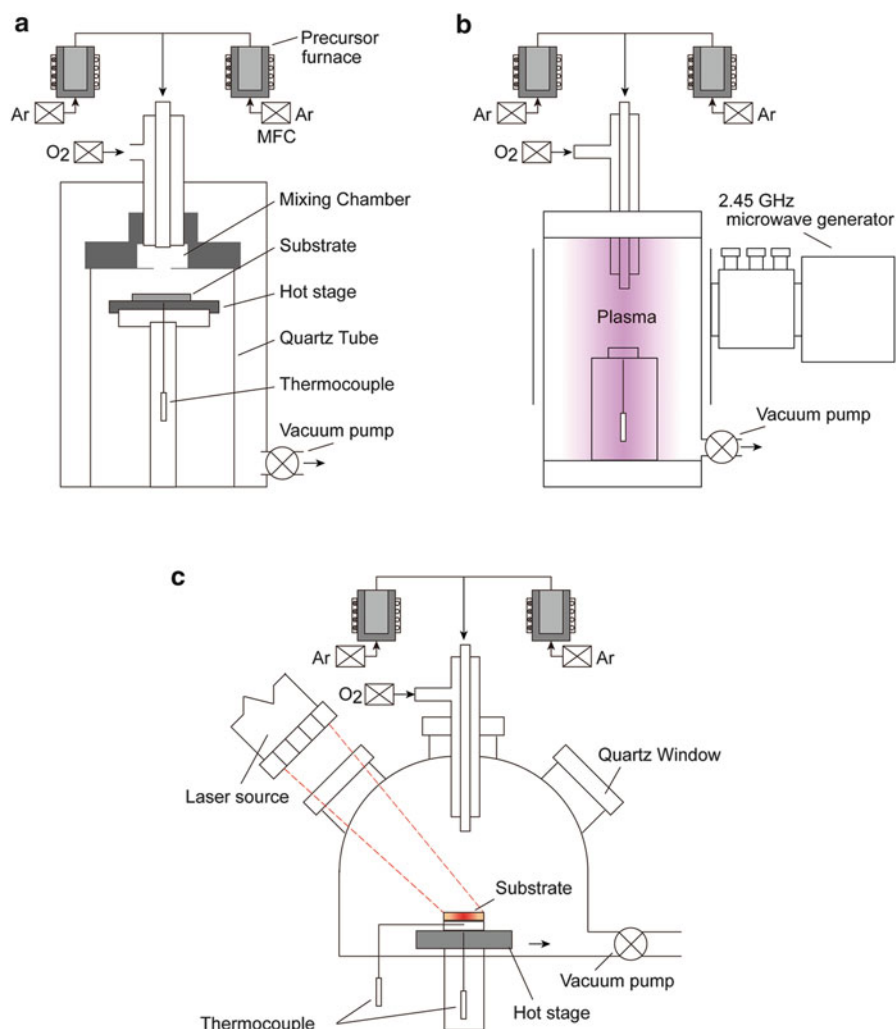


Fig. 9.1 Schematic diagram of thermal CVD (a), plasma enhanced CVD (PECVD) (b) and laser CVD (LCVD) (c)

high energy laser, typically an ultra-violet or Excimer laser, has the advantage of low temperature deposition without thermal degradation of the substrate. However, photolytic LCVD cannot create a wide-area coating at a high deposition rate. In pyrolytic LCVD, infra-red lasers, such as CO₂ and Nd:YAG lasers, are generally used. Pyrolytic LCVD heats locally at a small area of the substrate by focusing the laser beam; thus, source gases can easily access the heated area. The deposition rate of pyrolytic LCVD can be significantly high, reaching several 100 m/h [6]. However, the deposition area is usually less than several mm². Therefore, pyrolytic LCVD are generally understood to not make large-area coatings on substrates with

complicated shape. The authors first developed LCVD to prepare oxide and non-oxide films at high deposition speeds (more than several 100 $\mu\text{m/h}$) on wide-area substrates (around several cm^2) by using a high power laser (several 100 W of CO_2 , Nd:YAG and diode lasers), as shown later [11, 12].

9.3 CVD of Ca–P–O Films and Their Bio-Characteristics

Figure 9.2 depicts the phase diagram of a Ca–P–O system [13], which contains various bio-ceramic materials. α - and β - $\text{Ca}_3\text{P}_2\text{O}_8$ (TCP; tricalcium phosphate) have been widely studied as bio-resorbable materials. Figure 9.3 depicts the crystal structures of α - and β -TCP. The structure of α -TCP (Fig. 9.3a) is classified as a glaserite-type structure, where Ca ions exhibit coordination numbers ranging from five to nine and share edges with a PO_4 group [14]. Ca and phosphate ions are packed in columns along the c -axis in two ways; one contains only cations and the other contains both cations and anions. While the α -TCP is thermo-dynamically stable at 1,393–1,743 K and metastable at room temperature, β -TCP is stable below 1,393 K. The structure of β -TCP (Fig. 9.3b) is related to that of $\text{Ba}_3(\text{VO}_4)_2$, although β -TCP has lower symmetry due to site vacancies and distortions [15]. Ca ions coordinated to six, seven, eight and nine oxygen ions share edges with PO_4 tetrahedra. The major difference in crystal structure between α - and β -TCP is that

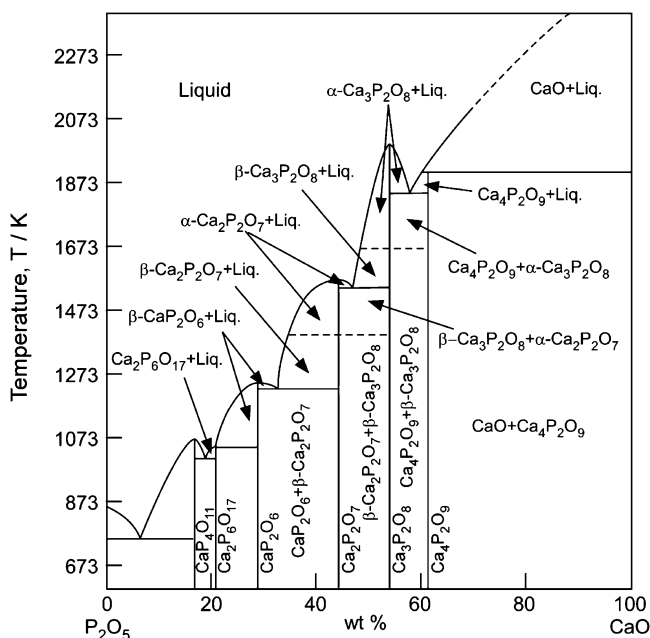


Fig. 9.2 A phase diagram of Ca–P–O system

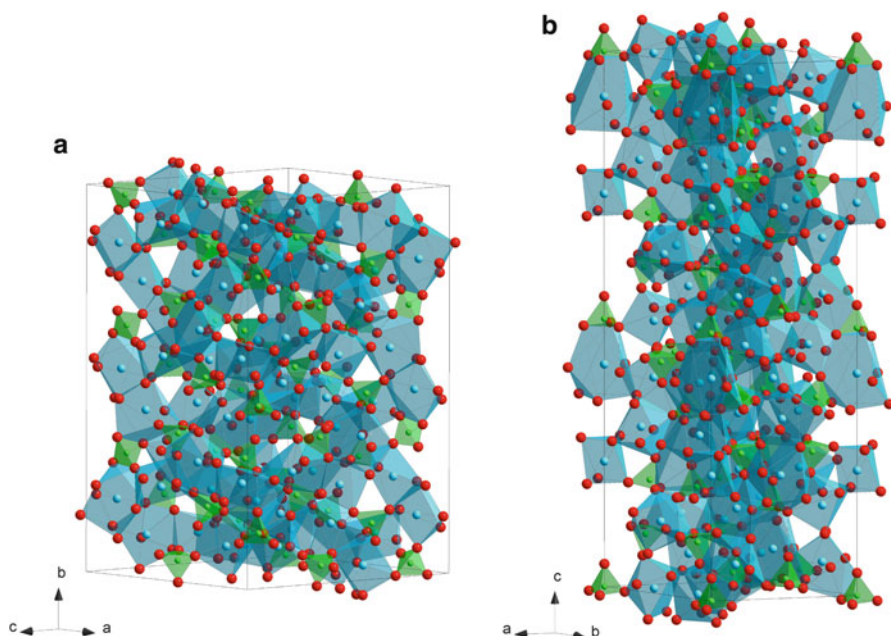


Fig. 9.3 Crystal structures of α - (a) and β -tricalcium phosphate (TCP) (b)

β -TCP has no cation–cation columns. Additionally, compared to that of β -TCP, α -TCP has a higher internal energy because of its higher volume per formula unit, which is consistent with α -TCP being the high-temperature phase [14].

α - and β - $\text{Ca}_2\text{P}_2\text{O}_7$ (CPP: calcium pyrophosphate) have been scarcely studied. The crystal structures of α - and β -CPP are illustrated in Fig. 9.4a, b, respectively. Structures of both α - and β -CPP contain pyro-groups, P_2O_7 , which consist of two corner-shared PO_4 tetrahedra with P–O–P angles of 130° for the α -phase and angles of 131° and 135° for the β -phase [16, 17]. In α -CPP, Ca ions coordinates with eight oxygen atoms and the chains of edge-shared Ca polyhedra form sheets parallel and perpendicular to the ac plane. The coordination numbers of Ca in β -CPP are seven, eight and nine; each pyrophosphate group is linked by commonly-shared Ca atoms, forming infinite pyrophosphate–Ca chelate-like chains [17]. Allen et al. prepared an α -CPP film by thermal CVD using $\text{Ca}(\text{dpm})_2$ (dpm: dipivaloylmethanate) and P_2O_5 at a total pressure (P_{tot}) of 1 kPa and a deposition temperature of 1,123 K. The β -CPP film was heat-treated at 1,623 K and transformed to a β -TCP film [18].

$\text{Ca}_4\text{P}_2\text{O}_9$ (TTCP: tetracalcium phosphate) would be more bio-resorbable than TCP because of its greater P_2O_5 content. TTCP is also written as $\text{Ca}_4(\text{PO}_4)_2\text{O}$ (tetracalcium diphosphate monoxide) since its structure contains Ca ions coordinated with seven and eight oxygen atoms that share PO_4 edges, and oxygen ions strongly coordinated to four Ca ions, forming tetrahedra of OCa_4 , as oxide ions (Fig. 9.5a) [19]. The Ca and P atoms lie near four sheets that contain two cation–anion (Ca–PO_4) columns and one cation–cation (Ca–Ca) column perpendicular

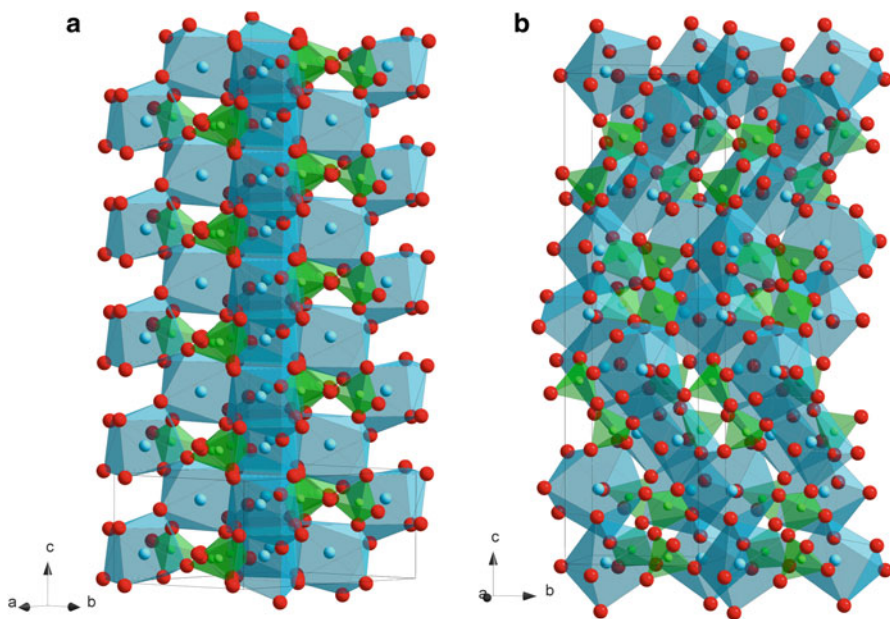


Fig. 9.4 Crystal structures of α - (a) and β -calcium pyrophosphate (CPP) (b)

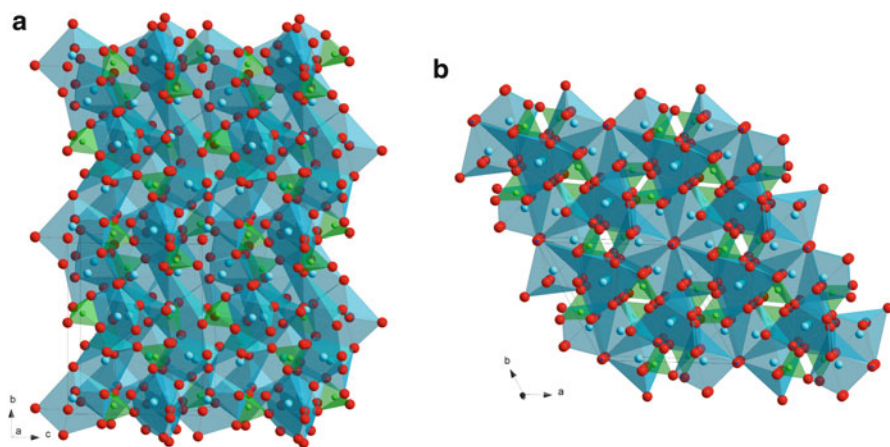


Fig. 9.5 Crystal structure of tetracalcium phosphate (TTCP) (a) calcium hydroxyapatite (HAp) (b)

to the b -axis. Because of these so-called ‘apatitic layers’, TTCP has a close structural relationship with calcium hydroxyapatite (HAp: $\text{Ca}_{10}(\text{PO}_4)_6(\text{OH})_2$) and its dehydration product, calcium oxyapatite (OAp: $\text{Ca}_{10}(\text{PO}_4)_6\text{O}$) [19–22].

Figure 9.5b depicts a crystal structure of HAp, which is illustrated by tetrahedra of PO_4 and polyhedra of Ca ions coordinated with seven and nine oxygen atoms.

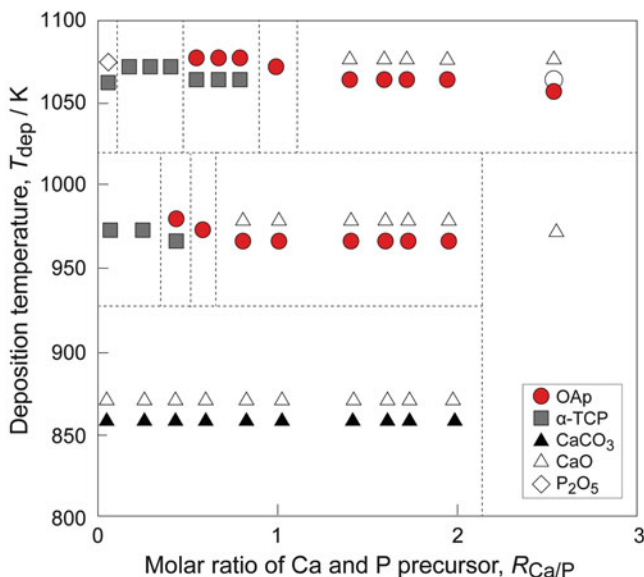


Fig. 9.6 Relationship between deposition parameters and crystal phases by thermal CVD

HAp and OAp have ‘apatite layers’, composed of two $Ca-PO_4$ columns and one Ca-Ca column parallel to the *ac* plane, and hydroxyl ions in HAp and oxygen ions in OAp are located at the center of Ca hexagons parallel to the *ab* plane. HAp or OAp have been frequently studied because HAp is bio-active and similar to human bones. Although many techniques including solid-state sintering, sol-gel and magnetron sputtering [23] have been employed to prepare OAp or HAp, Darr et al. prepared fluorine-containing carbonated hydroxyapatite by thermal CVD using $Ca(tmhd)_2$ (where $tmhd=2,2,6,6$ -tetramethylheptane-3,5-dione) and P_2O_5 [24]. The crystal structure of the film was not investigated, but the Ca/P content of the film was about 1.3 which is different from that of HAp ($Ca/P=1.7$). The bio-compatibility of this film was not reported. Since OH is easily evaporated in a vacuum, preparing OH-containing HAp by dry processes (vacuum processes), such as CVD and sputtering, is difficult. OAp film prepared by magnetron sputtering did not contain OH [25], whereas OAp film prepared by thermal CVD contained a small amount of OH. In this review, the OAp film prepared by CVD containing a small amount of OH is described as OAp film. The authors first prepared a crystalline OAp film in as-deposited form.

By controlling deposition parameters, various bio-ceramic films of TCP, TTCP and OAp films can be prepared by thermal CVD. Figure 9.6 represents the relationship between deposition parameters and crystal phases, i.e., the CVD phase diagram, by thermal CVD using $Ca(dpm)_2$ and $(C_6H_5O_3)PO$ as source materials [5]. α -TCP film in a single phase can be prepared at a high deposition temperature (T_{dep}) and low Ca/P gas ratio ($R_{Ca/P}$), while OAp film in a single phase can be prepared at a

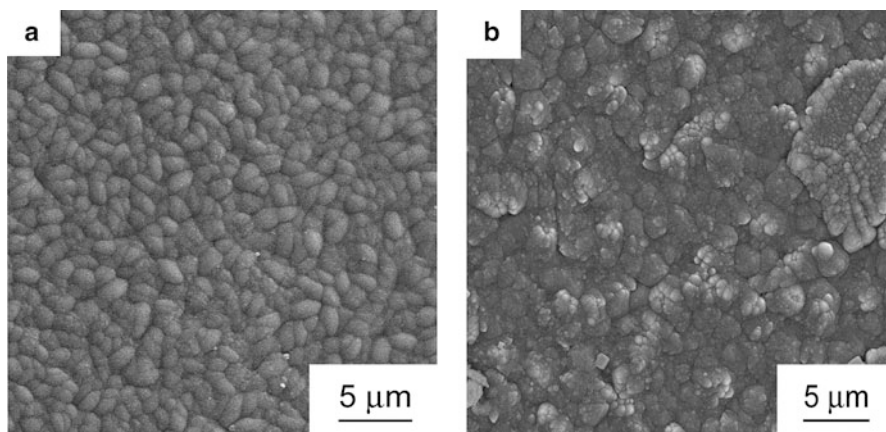


Fig. 9.7 Surface morphology of α -TCP (a) and OAp (b) films prepared by thermal CVD

high T_{dep} and intermediate $R_{\text{Ca/P}}$ condition. Figure 9.7a, b depict the surface morphologies of α -TCP and OAp films in a single phase, respectively. The α -TCP film has uniform and smooth small grains, while the OAp film has a cauliflower structure. Figure 9.8 shows the HAp regeneration behavior in Hanks' solution on the α -TCP film [26]. A small amount of HAp embryo starts to form after 1 day of immersion, and the whole surface of the α -TCP film is covered by HAp after 14 days. Figure 9.9 shows the HAp regeneration behavior in Hanks' solution on the OAp film. The HAp embryo formed within a 1 h, and the whole surface is covered by HAp within 6 h. HAp regeneration is preferential at hollows in the cauliflower-like grains. HAp and OAp have hexagonal structures as shown in Fig. 9.5b. HAp regeneration is also preferred to c -axis on the c -plane. The preferential c -axis orientation of the OAp film can be obtained by controlling T_{dep} and $R_{\text{Ca/P}}$ in thermal CVD. The highly c -axis oriented OAp film exhibited the highest regeneration of HAp in Hanks' solution [27]. Since a few months are needed for bone regeneration on Ti without bio-ceramic coatings, the OAp coating by thermal CVD is the effective strategy to regenerate HAp.

Since lasers can photolytically or thermally activate source gases, more kinds of Ca-P-O materials can be prepared by LCVD. Figure 9.10a, b depict the relationship between deposition parameters and the crystal phases (CVD phase diagram) by LCVD using $\text{Ca}(\text{dpm})_2$ and $(\text{C}_6\text{H}_5\text{O}_3)\text{PO}$ as source gases at a low (30 W) and high (200 W) laser power, respectively [28]. At relatively low T_{dep} of 750–950 K, a mixture film of OAp and β -TCP or OAp and TTCP can be obtained under a wide range of conditions. OAp films in a single phase can be obtained at $R_{\text{Ca/P}} = 0.5$ to 0.6. At T_{dep} of 1,000–1,300 K, a mixture film of OAp and α -TCP can be prepared by LCVD. α -TCP films can be prepared by thermal CVD, whereas both α - and β -TCP films can be prepared by LCVD.

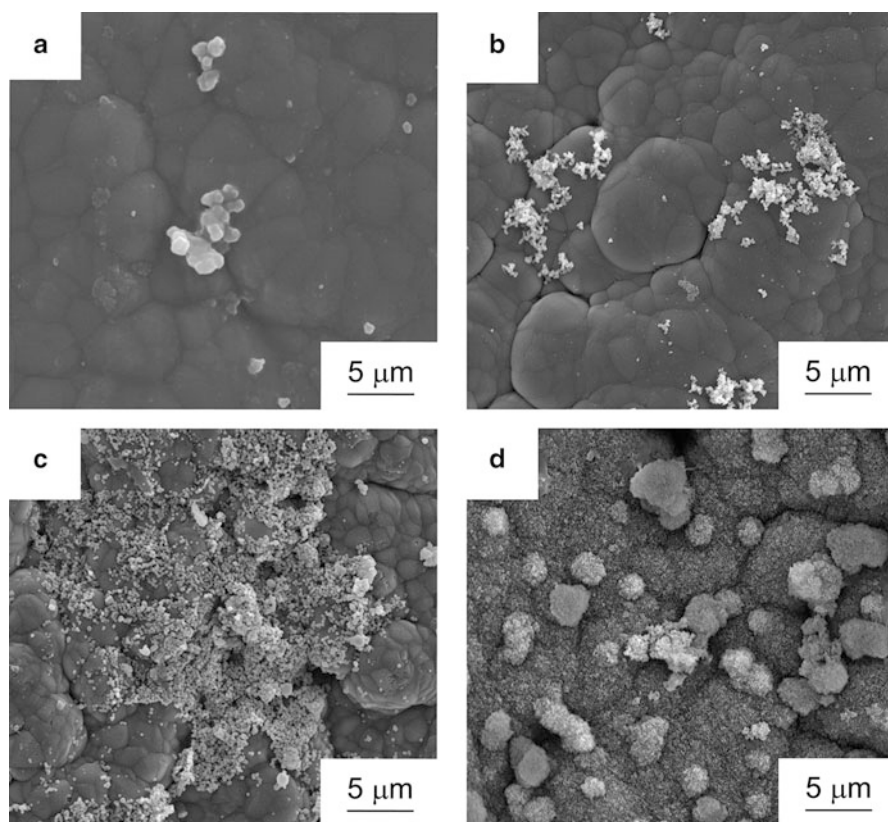


Fig. 9.8 HAP regeneration behavior on α -TCP film in Hanks' solution for 1 day (a), 3 days (b), 7 days (c) and 14 days (d)

Plasma can electromagnetically activate source gases, and a greater variety of Ca-P-O system materials can be synthesized by PECVD. Figure 9.11 depicts the relationship between deposition parameters and crystal phases (the CVD phase diagram) by PECVD using $\text{Ca}(\text{dpm})_2$ and $(\text{C}_6\text{H}_5\text{O}_3)\text{PO}$ as source gases. α - and β -CPP films can both be prepared by PECVD. At a relatively high T_{dep} , a β -CPP film in a single phase or a mixture film of β -CPP and α -TCP can be prepared. At a low T_{dep} , a mixture of β - and α -TCP can be prepared. Figure 9.12 shows change in surface morphology of a β -CPP film prepared at micro-wave power of 4 kW and $R_{\text{Ca/P}} = 0.7$ after immersion in Hanks' solution. A slightly smooth surface morphology can be seen after immersion for 3 days, suggesting that β -CPP is bio-resorbable. A small amount of HAP embryo can be observed after immersion for 7 days.

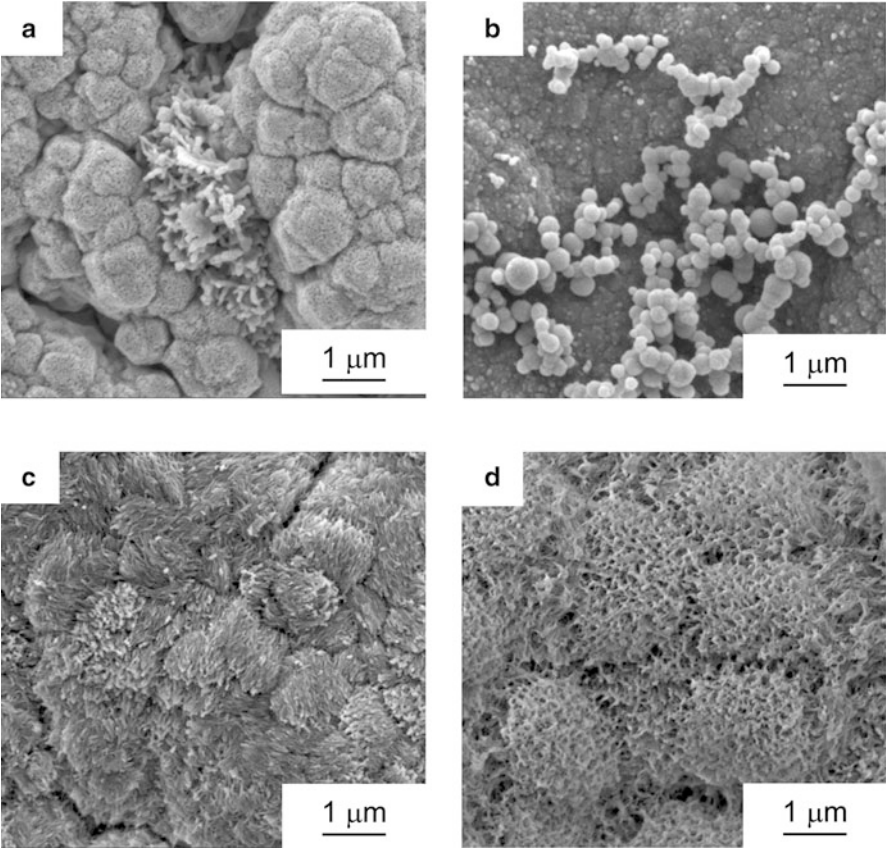


Fig. 9.9 Hap regeneration behavior on OAp film in Hanks' solution for 1 h (a), 3 h (b), 6 h (c) and 12 h (d)

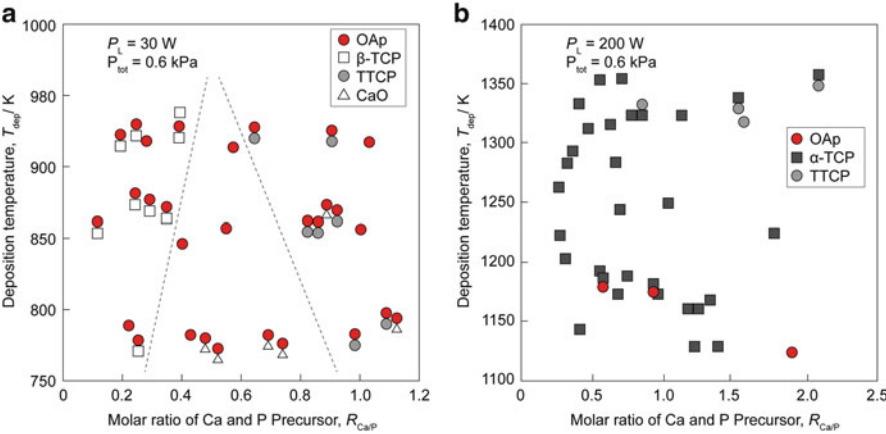


Fig. 9.10 Relationship between deposition parameters and crystal phases by LCVD at a low (a) and high (b) laser power

Fig. 9.11 Relationship between deposition parameters and crystal phases by PECVD

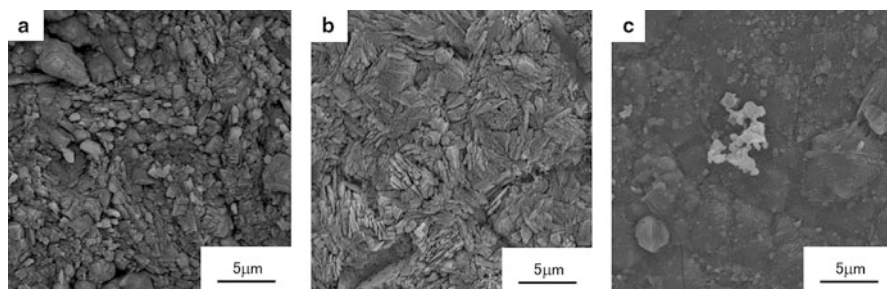
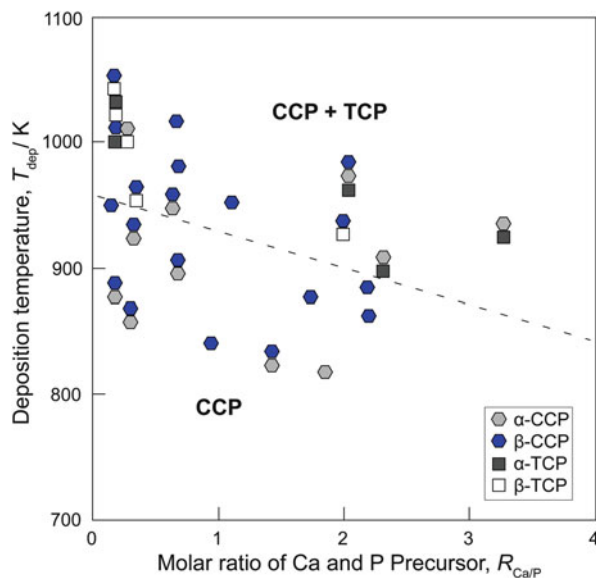


Fig. 9.12 HAp regeneration behavior on CPP film in Hanks' solution for 1 day (a), 3 days (b), 7 days (c)

9.4 Summary

CVD is a promising process for bio-ceramic coatings because it can provide well-defined crystal phases and microstructures through the control of process parameters. Auxiliary energy sources, such as laser and plasma, are particularly useful to fabricate materials that cannot be synthesized by conventional thermal CVD. The Ca-P-O system has many useful bio-ceramics, i.e., bio-inert, bio-active and bio-resorbable materials. CVD and in particular LCVD and PECVD are promising methods for the preparation of metastable or unstable bio-ceramic materials. Since CVD has many process parameters, CVD can prepare optimized microstructures, crystal phases and preferential orientations for HAp regeneration.

Open Access This chapter is distributed under the terms of the Creative Commons Attribution Noncommercial License, which permits any noncommercial use, distribution, and reproduction in any medium, provided the original author(s) and source are credited.

References

1. Goto T, Narushima T, Ueda K. Biological and biomedical coatings handbook-processing and characterization. Boca Raton: CRC; 2011.
2. Powell CF. Chemical vapor deposition. In: Powell CF, Oxley JH, Blocher Jr JM, editors. Vapor deposition. New York: Wiley; 1966. p. 249–76.
3. Sato M, Tu R, Goto T. Preparation conditions of CaTiO_3 film by metal-organic chemical vapor deposition. *Mater Trans.* 2006;47:1386–90.
4. Nath S, Tu R, Goto T. Preparation of Ca–Si–O films by chemical vapor deposition. *Surf Coating Tech.* 2010;205:2618–23.
5. Sato M, Tu R, Goto T. Preparation of hydroxyapatite and calcium phosphate films by MOCVD. *Mater Trans.* 2007;48:3149–53.
6. Duty C, Jean D, Lackey WJ. Laser chemical vapor deposition: materials, modeling, and process control. *Int Mater Rev.* 2001;46:271–87.
7. Preauchat B, Drawin S. Properties of PECVD-deposited thermal barrier coatings. *Surf Coating Tech.* 2001;142–144:835–42.
8. Hirai T, Goto T, Kaiji T. Preparation of silicon carbide by chemical vapor deposition. *J Ceram Soc Jpn.* 1983;91:503–9.
9. Tu R, Goto T. High temperature stability of anastase films prepared by MOCVD. *Mater Trans.* 2008;49:2040–6.
10. Zhang W, Vargas R, Goto T, Someno Y, Hirai T. Preparation of epitaxial AlN films by electron cyclotron resonance plasma-assisted chemical vapor deposition on Ir- and Pt-coated sapphire substrates. *Appl Phys Lett.* 1994;64:1359–61.
11. Goto T, Banal R, Kimura T. Morphology and preferred orientation of Y_2O_3 film prepared by high-speed laser CVD. *Surf Coating Tech.* 2007;201:5776–81.
12. Goto T. Thermal barrier coatings deposited by laser CVD. *Surf Coating Tech.* 2005;198:367–71.
13. Hill WL, Faust GT, Reynolds DS. The binary system P_2O_5 – 2CaO – P_2O_5 . *Am J Sci.* 1944;242:457–77.
14. Mathew M, Schroeder LW, Dickens B, Brown WE. The crystal structure of $\alpha\text{-Ca}_3(\text{PO}_4)_2$. *Acta Crystallogr.* 1977;B33:1325–33.
15. Dickens B, Schroeder LW, Brown WE. The crystal structure of pure $\beta\text{-Ca}_3(\text{PO}_4)_2$. *J Solid State Chem.* 1974;10:232–48.
16. Calvo C. The crystal structure of $\alpha\text{-Ca}_2\text{P}_2\text{O}_7$. *Inorg Chem.* 1968;7:1345–51.
17. Webb NC. The crystal structure of $\beta\text{-Ca}_2\text{P}_2\text{O}_7$. *Acta Crystallogr.* 1966;21:942–8.
18. Allen GC, Ciliberto E, Fragala I, Spoto G. Surface and bulk study of calcium phosphate bioceramics obtained by Metal Organic Chemical Vapor Deposition. *Nucl Instrum Methods B.* 1996;116:457–60.
19. Dickens B, Brown WE, Kruger GJ, Stewart JM. $\text{Ca}_4(\text{PO}_4)\text{O}$, tetracalcium diphosphate monoxide. Crystal structure and relationships to $\text{Ca}_5(\text{PO}_4)_3\text{OH}$ and $\text{K}_3\text{Na}(\text{SO}_4)_2$. *Acta Crystallogr.* 1973;B29:2046–56.
20. Kay MI, Young RA. Crystal structure of hydroxyapatite. *Nature.* 1964;204:1050–2.
21. Henning PA, Landa-Canovas AR, Larsson A, Lidin S. Elucidation of the crystal structure of oxyapatite by high-resolution electron microscopy. *Acta Crystallogr.* 1999;B55:170–6.
22. Elliott JC. Structure and chemistry of the apatites and other calcium orthophosphates. Amsterdam: Elsevier; 1994.

23. Narushima T, Ueda K, Goto T, Masumoto H, Katsube T, Kawamura H, Ouchi C, Iguchi Y. Preparation of calcium phosphate films by radiofrequency magnetron sputtering. *Mater Trans.* 2005;46:2246–52.
24. Darr JA, Guo ZX, Raman V, Bououdina M, Rehman IU. Metal organic chemical vapour deposition (MOCVD) of bone mineral like carbonated hydroxyapatite coatings. *Chem Commun.* 2004;6:696–7.
25. Ueda K, Narushima T, Goto T, Katsube T, Nakagawa H, Kawamura H, Taira M. Evaluation of calcium phosphate coating films on titanium fabricated using RF magnetron sputtering. *Mater Trans.* 2007;48:307–12.
26. Sato M, Tu R, Goto T, Ueda K, Narushima T. Hydroxyapatite formation on Ca–P–O coating prepared by MOCVD. *Mater Trans.* 2008;49:1848–52.
27. Sato M, Tu R, Goto T, Ueda K, Narushima T. Apatite formation behavior on bio-ceramic films prepared by MOCVD. *J Ceram Soc Jpn.* 2009;117:461–5.
28. Sato M, Tu R, Goto T, Ueda K, Narushima T. Preparation behavior in a Hanks' solution on Ca–P–O films prepared by laser CVD. *Mater Trans.* 2009;50:2455–9.